

Invisibility assessment: a visual perception approach

Ivan Moreno,^{1,*} Y. Jauregui-Sánchez,² and Maximino Avendaño-Alejo³

¹Unidad Académica de Física, Universidad Autónoma de Zacatecas, Zacatecas 98060, Mexico

²Instituto Nacional de Astrofísica, Óptica y Electrónica, Puebla 72840, Mexico

³Universidad Nacional Autónoma de México, Centro de Ciencias Aplicadas y Desarrollo Tecnológico, D.F. 04510, Mexico

*Corresponding author: imoreno@fisica.uaz.edu.mx

Received March 18, 2014; revised July 24, 2014; accepted August 22, 2014;
posted August 25, 2014 (Doc. ID 208362); published September 19, 2014

Determining the invisibility of an optical cloak intended to hide something has become a complex problem in recent years. There are many invisibility mechanisms, the performance is quite different from technique to technique, and it is desirable to have a precise metric for their comparison. Here, we propose a simple metric that assesses the perceived invisibility. This invisibility index is based on the fact that the human visual system (HVS) is highly sensitive to spatial frequencies, and then uses the Fourier transform and the contrast sensitivity function of the HVS to assess invisibility. © 2014 Optical Society of America

OCIS codes: (230.3205) Invisibility cloaks; (330.5000) Vision - patterns and recognition; (120.4820) Optical systems; (230.0230) Optical devices; (100.4999) Pattern recognition, target tracking; (330.7310) Vision.
<http://dx.doi.org/10.1364/JOSAA.31.002244>

1. INTRODUCTION

The quest for invisibility has made great progress in recent years [1–9]. Invisibility techniques range from mimesis and camouflaging to modern optical devices, such as electromagnetic cloaking in the visible spectrum (Fig. 1).

Up to now, the performance of invisibility cloaking has been judged by qualitative assessment [10,11]. For example, in electromagnetic cloaking only the perturbation of the light path or the wavefront shape is examined. However, as invisibility cloaking methods are getting more advanced, it is becoming important to quantitatively assess how good the cloaking performance of invisibility devices is. With such a measure, one could quantitatively test and compare different cloaking approaches. Here, we propose a simple invisibility metric based on the human visual system (HVS).

The notion of invisibility is strongly related to human visual perception. For humans, invisibility is a psychological phenomenon experienced when seeing or perceiving a particular object in certain scenery. The invisibility of an optical cloak intended to hide something depends on the perturbation of the visual field. Such perturbation may have visual attributes, like blurring, distortion, and transparency change. Transparency is the visual property of seeing something through something else, without seeing what is in front but seeing what is behind, along the same line of sight. Distortion is visually manifested by changes in the shape of objects, i.e., the true geometry of an object in the visual field is not maintained in the perceived scene. And blurring decreases the sharpness of the visual field, i.e., induces faults in the object details of a visual scene that is being observed.

The cloak optics allows, to some degree, for light to pass through without apparent reflection, refraction, and absorption. But how the cloak deals with light is just one factor. Invisibility perception depends on several factors (Fig. 2): the HVS, the cloak optics, the background scenery, and

distraction factors [12]. The relationship among all of them determines the degree of invisibility that is visually perceived. Therefore, when assessing invisibility cloaks, a metric of invisibility should ideally incorporate all these factors.

2. ASSESSMENT WITH CROSS CORRELATION

As far as we know, there is only one invisibility metric, which was recently proposed by Halimeh *et al.* [13]. It is the cross correlation function, which statistically assesses the similarity between two images, A and B . Image A contains an “invisible” object, and B is the image of reference, which is the same image, but without the “invisible” object. The calculation of the correlation function for images is done by means of the normalized cross correlation (NCC), which is a simple merit function that is used in image pattern recognition [14]. The NCC between two images, A and B , is

$$\text{NCC} = \frac{\sum_i^M (A_i - \bar{A})(B_i - \bar{B})}{\sqrt{\sum_i^M (A_i - \bar{A})^2 \sum_i^M (B_i - \bar{B})^2}}, \quad (1)$$

where $i = 1, 2, \dots, M$, and the image size in pixels is M . \bar{A} and \bar{B} are the mean of A and B across all image pixels. As the cloak in A is more invisible, the similarity between A and B increases, and NCC approaches 1. An NCC equal to 1 means that the cloak in A is perfectly invisible.

The NCC is a simple approach that involves numeric values of brightness, and then retrieves invisibility information at the lowest level of human vision. But, in most cases, invisible cloaks are ultimately to be hidden from human beings and then their assessment should be through higher levels of human perception.

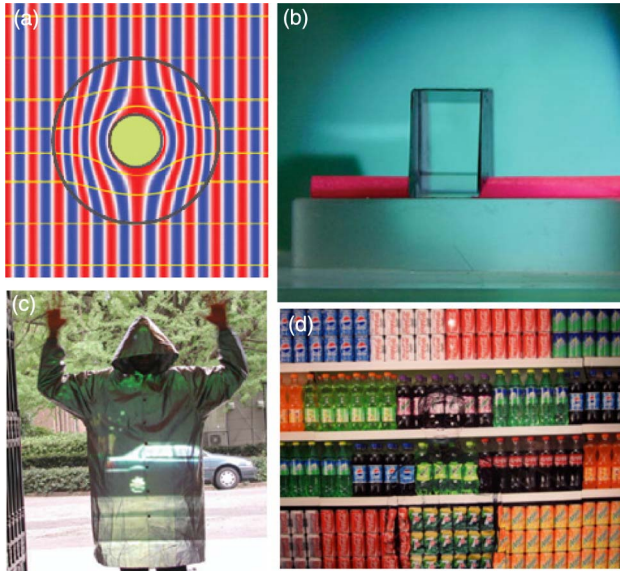


Fig. 1. Four examples of invisibility techniques. (a) Cylindrically shaped electromagnetic cloak [1], (b) Calcite cloak hiding the central part of a piece of pink-colored paper [3], (c) Tachi's virtual invisibility cloak by retroreflective projection technology [4], and (d) artistic invisibility of Bolin [5].

3. NEW INVISIBILITY METRIC

One of the main functions of the human vision is to extract structural information from the viewing field, and the HVS is highly adapted for this purpose [15]. For example, two different cloaks could have the same NCC, but one of them be perceived more invisible because the visual perception of its spatial structure. A realistic metric should be sensitive to the spatial structure of the cloak and the background. However, HVS models are too complex to implement in a simple equation.

Here we propose a simple metric that takes into account the structural information of the field of view. In analogy to the “spot the differences” game, in the Fourier domain, we compute the “visible” differences in the spatial frequencies space (VDF), and use it for weighting the NCC. We propose an invisibility quotient (IQ) given by

$$IQ = \frac{NCC}{1 + k \cdot VDF^\alpha}, \quad (2)$$

where NCC is calculated by Eq. (1), k is a constant that fits the range of IQ, and α adjusts the relative weight of VDF. Throughout this paper, the IQ parameter setting is $k = 1$ and $\alpha = 2$. These values, k and α , are chosen so that IQ approximates the perceived invisibility: α because VDF seems to be nonlinear with perception, and k for simplicity. A value of IQ = 1 means that the cloak in image A is perfectly invisible. In this metric, the NCC is multiplied by a factor that weights its relevance for the HVS, the $(1 + VDF^2)^{-1}$.

To define VDF, we consider the HVS ability to perceive gray level differences in visual sceneries as function of spatial frequencies, i.e., we use the contrast sensitivity function (CSF) of the HVS (Fig. 3). We weight the difference between the spatial frequency spectra of images, A (with “invisible” object), and B (without “invisible” object), with the CSF, and we define VDF as the ratio of visible spatial frequency differences to the total visible spatial frequencies in the scene image, i.e., [16],

$$VDF = \frac{\sum_{n=1}^N CSF(\omega_n) |F_A(\omega_n) - F_B(\omega_n)|}{\sum_{n=1}^N CSF(\omega_n) F_A(\omega_n)}, \quad (3)$$

where ω_n is the n th angular spatial frequency. Number N determines the number of visible spatial frequencies, i.e., $\omega_N < 50$ cpd (cycles per degree), approximately [17–19]. $F_A(\omega_n)$ and $F_B(\omega_n)$ are the complex modulus of the discrete Fourier transform (power spectrum) of images, A and B , and we set $F_A(0) = F_B(0) = 0$.

The CSF describes the sensitivity of the HVS to different spatial frequencies that are present in the visual field (Fig. 3). Here we use the CSF Daly model [19], which is a function of radial spatial frequency, viewing angle, brightness level (Weber's Law), viewing distance, and size of the viewing field area. It is

$$CSF(\omega) = \min \left[CSF_0(\omega), CSF_0 \left(\frac{\omega}{r_a r_\theta} \right) \right], \quad (4)$$

where “ $\min[b, c]$ ” is the minimum between b and c , and

$$CSF_0(\omega) = 0.9A_L \omega e^{-0.9B_L \omega} [351.57[\omega^2 A_p]^{-1.5} + 1]^{-0.2} \times [1 + 0.06e^{0.9B_L \omega}]^{0.5},$$

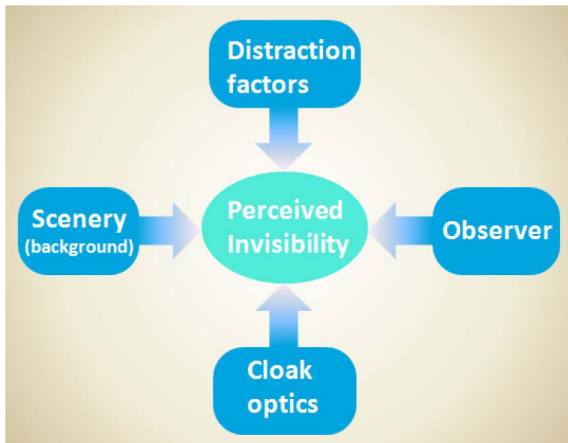


Fig. 2. Perceived invisibility depends on several factors. How the optical cloak deals with light is just one factor. The HVS of observer, distractions in the environment, and the background scenery also have an important influence on the perceived invisibility.

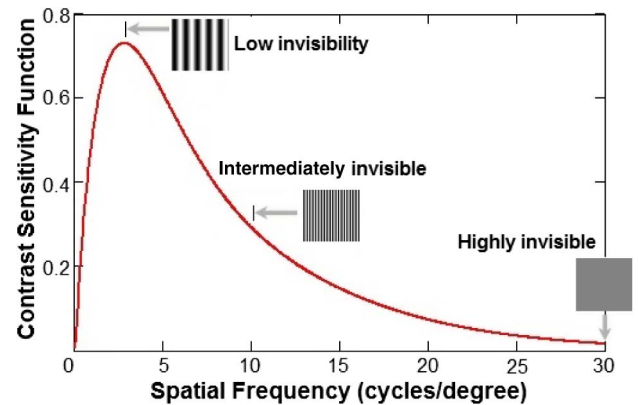


Fig. 3. CSF represents the contrast perceptibility of a periodic pattern as a function of its spatial frequency. The three fringe patterns illustrate the contrast invisibility for different spatial frequencies.

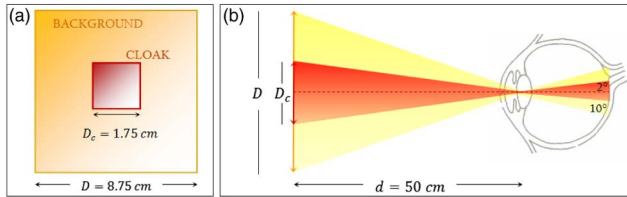


Fig. 4. Geometrical details for both invisibility calculation and visual display. (a) Shows the size of both image background and the cloak placed at the center, where $D \times D$ is image size and $D_C \times D_C$ is cloak size. (b) Shows the observation distance d , and angles subtended at the eye's retina. All images analyzed are of 512×512 pixels.

where A_p is the area of the viewing field in square degrees. The other parameters are: $A_L = 0.801(1 + 0.7/L)^{-0.2}$, $B_L = 0.3(1 + 100/L)^{0.15}$, $r_a = 0.856d^{0.14}$, and $r_\theta = 0.11 \cos(4\theta) + 0.89$. Here, L is the light adaptation level in cd/m^2 , d is the viewing distance in meters, and θ is the viewing angle in degrees. Equation (4) has a discontinuity in $\omega = 0$, then it is defined as $\text{CSF}(0) = 0$.

To illustrate the potential of IQ, we analyze several invisibility cloaks in several background scenarios. Geometrical details for both invisibility calculation and visual display are shown in Fig. 4. The viewing distance was set so that the invisibility cloak subtended 2 deg, and the entire image subtended 10 deg. This is because, at typical viewing distances, only a local area in the image can be perceived with high resolution by the human observer (the fixation point, which corresponds to the center of the eye's retina, the fovea). Other parameters are: front view ($\theta = 0$), observation distance, $d = 50$ cm, viewing field area, $A_p = 10^\circ \times 10^\circ$, and the image displayed at luminance, $L \sim 150 \text{ cd}/\text{m}^2$ (mean L of a laptop screen).

Figure 5 shows the invisibility cloaks we analyzed, which illustrate the basic visual disturbances due to invisibility cloaks: blurring, distortion, and transparency change. These visual disturbances of the background were created by image processing. Whirl is a transparent distortion of image, Lines is a periodic variation of transparency, and Diffuse is a smoothing of background.

Figure 6 shows the Whirl cloak in two different image backgrounds. By using NCC, the invisibility in Fig. 6(a) is 99%, which is higher than the invisibility of Fig. 6(b) with $\text{NCC} = 98.8\%$. However, the perceived invisibility degree of Fig. 6(a) is lower than that of Fig. 6(b). The IQ is in agreement with visual perception because $\text{IQ} = 95.26\%$ in Fig. 6(a), which is lower than in Fig. 6(b), where $\text{IQ} = 97.95\%$.

Figure 7 shows two cloaks (Diffuse and Lines) in the same background, both with identical NCC. However, Fig. 7(a) is perceived less invisible than Fig. 7(b). The IQ in Fig. 7(a) is $\text{IQ} = 90.91\%$, which is lower than in Fig. 7(b) with $\text{IQ} = 97.48\%$. As shown in Figs. 6 and 7, the metric IQ approaches



Fig. 5. Images with the invisibility cloaks we used in the analysis. From left to right the cloaks are: Diffuse, Whirl, and Lines. In these images, for illustration purposes, a frame surrounds the cloak.



Fig. 6. Invisibility assessment of Whirl cloak in two different backgrounds. By using cross correlation, the invisibility in (a) should be higher ($\text{NCC} = 99\%$) than in (b) where $\text{NCC} = 98.8\%$. However, (a) is perceived as less invisible than (b). The IQ in image (a) is $\text{IQ} = 95.26\%$, which is lower than in (b) with $\text{IQ} = 97.95\%$. (c) and (d) are the background images without the invisibility cloak.

the visual perception better than the NCC. The advantage of IQ is that it somehow incorporates 3 of the main factors of invisibility perception (scenery, cloak optics, and observer), while NCC incorporates only 2 factors (scenery and cloak optics).

4. MEAN INVISIBILITY QUOTIENT

The invisibility calculated by both NCC and IQ changes when the cloak is presented against different backgrounds. Image distortions caused by the cloak depend on the local image statistics and structure. But a single overall quality measure of invisibility, independent from the background, may be desirable in practice. Such an intrinsic invisibility may be obtained by computing IQ over a wide range of backgrounds with different spatial structures. For this purpose, we propose a mean invisibility quotient (MIQ) as follows:

$$\text{MIQ} = \frac{1}{S} \sum_{j=1}^S \text{IQ}_j, \quad (5)$$

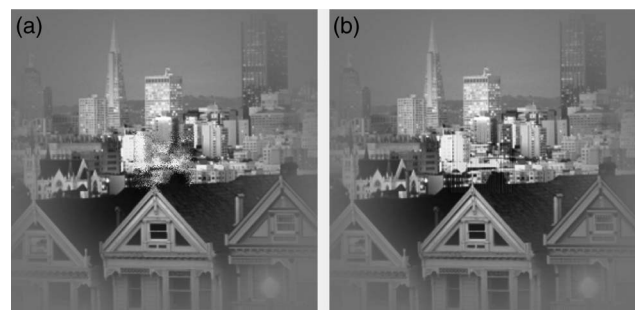


Fig. 7. Invisibility assessment of two cloaks (Diffuse and Lines) in the same background, both with identical $\text{NCC} = 97.7\%$. However, (a) is perceived as less invisible than (b). The IQ in image (a) is $\text{IQ} = 90.91\%$, which is lower than in (b), with $\text{IQ} = 97.48\%$.

where IQ_j is the cloak IQ at the j -th background image; and S is the number of backgrounds. With such an averaging approach, the invisibility assessment approximately characterizes an invisibility cloak independently from the image background. The number and variety of backgrounds may be too large, but for practical purposes it should be selectively limited. We propose six meaningful backgrounds ($S = 6$) with representative spatial structures: one human face, and five standard human vision stimuli, which we selected from the ModelFest stimuli (visual stimuli used to build the standard model for foveal detection of spatial contrast) [17,20]. The six backgrounds are: Lena face [21], a city view (stimuli 43), a 1D periodic pattern (stimuli 8), a radial periodic pattern (stimuli 41), a white-black pattern (stimuli 42), and a random structure pattern (stimuli 35). These image backgrounds constitute a set of representative spatial frequencies and structures.

To verify the effectiveness of this metric, we calculate the MIQ for the Diffuse, Whirl, and Lines cloak. The image distortion due to each cloak is created with an optical filter that has the same optical weight in the six background images, and is adjusted so that the average NCC of the three cloaks is identical. Figure 8 shows the three cloaks in the six different backgrounds. The mean NCC indicates that the three cloaks have equal invisibility, but they have different perceived invisibility. MIQ is in agreement with visual perception; i.e., Lines cloak is the most invisible with a MIQ = 95.58%, followed by the Whirl cloak with MIQ = 79.25%, and finally the Diffuse cloak with MIQ = 72.16%. Therefore, the advantage of MIQ is that it may discriminate different cloaks by its perceived invisibility. Then, MIQ could be an indicator of the intrinsic invisibility, which should change for different levels of transparency, distortion or blurring.

5. SUMMARY

We set a definition for perceived invisibility that accounts for the main factors that affect the invisibility performance. Using some of these factors, we have proposed a new metric for assessing invisibility based on the HVS. The new invisibility index is based on the fact that the HVS is highly sensitive to spatial frequencies, and then uses the Fourier transform and the CSF of the HVS in a simple and meaningful way. A single overall quality measure of invisibility, approximately independent from the background, was also proposed. The promise of the new invisibility index was demonstrated through three intuitive examples (Figs. 6–8). Because there are many invisibility mechanisms, and the performance is quite different from technique to technique, the proposed metric can provide a realistic quality assessment of the invisibility cloak, which delivers more information about the ultimate performance of the cloak and should lead to design strategies for performance improvement of invisibility devices.

There are a number of issues that deserve further investigation with regard to both invisibility indices IQ and MIQ. Several interesting questions arise. For example, in Eq. (5), how many backgrounds are necessary, should contributions from different backgrounds be weighted, and how should these weighting coefficients be chosen? About IQ calculation, it compares two 2D static images, but human eyes see a 3D world in movement. Perceived invisibility in 3D should be assessed, and movement may be incorporated in an invisibility index.

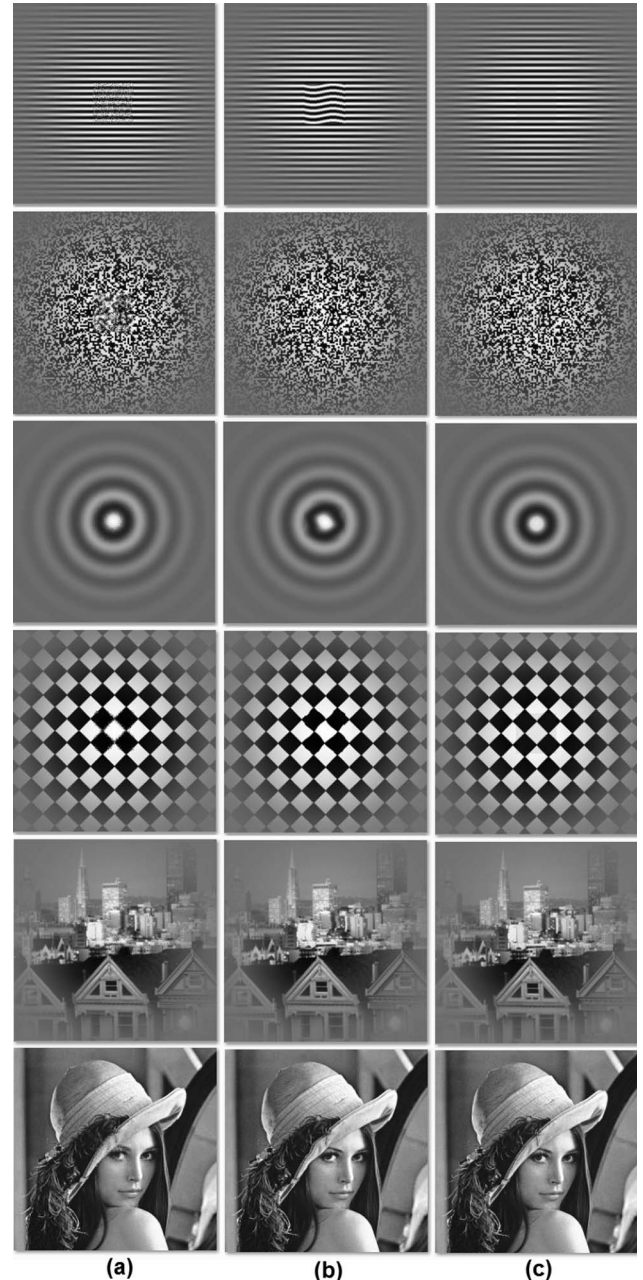


Fig. 8. Invisibility assessment of the three cloaks (Diffuse, Whirl, and Lines) using MIQ. The three cloaks have an identical mean NCC = 97.5%. However, on average, Diffuse cloak in (a) images is perceived less invisible than Whirl cloak in (b) images, and the cloak in (b) is perceived less invisible than Line cloak in (c).

ACKNOWLEDGMENTS

This research was supported by the Consejo Nacional de Ciencia y Tecnología (CONACYT) with grant 128452. We also thank the reviewers for their constructive and insightful comments and suggestions.

REFERENCES AND NOTES

1. W. Cai, U. K. Chettiar, A. V. Kildishev, and V. M. Shalaev, "Optical cloaking with metamaterials," *Nat. Photonics* **1**, 224–227 (2007).
2. J. Fischer, T. Ergin, and M. Wegener, "Three-dimensional polarization-independent visible-frequency carpet invisibility cloak," *Opt. Lett.* **36**, 2059–2061 (2011).

3. B. Zhang, Y. Luo, X. Liu, and G. Barbastathis, "Macroscopic invisibility cloak for visible light," *Phys. Rev. Lett.* **106**, 033901 (2011).
4. S. Tachi, "Telexistence and retro-reflective projection technology (RPT)," in *Proceedings of 5th Virtual Reality International Conference (VRIC 2003)*, pp. 69/1–69/9.
5. L. Bolin, "Hiding in the city No. 93 Supermarket No. 2—in pictures," www.kleinsungallery.com (2010).
6. J. C. Howell, J. B. Howell, and J. S. Choi, "Amplitude-only, passive, broadband, optical spatial cloaking of very large objects," *Appl. Opt.* **53**, 1958–1963 (2014).
7. R. Fleury and A. Alu, "Cloaking and invisibility: a review," *Forum Electromagn. Res. Methods Appl. Technol. (FERMAT)*, **1**, 1–24 (2014).
8. A. F. Nielsen, "The digital chameleon principle: computing invisibility by rendering transparency," *IEEE Comp. Graph. Appl.* **27**, 90–96 (2007).
9. F. Zambonelli and M. Mamei, "The cloak of invisibility: challenges and applications," *IEEE Pervasive Computing* **1**, 62–70 (2002).
10. A. J. Danner, "Visualizing invisibility: metamaterials-based optical devices in natural environments," *Opt. Express* **18**, 3332–3337 (2010).
11. C.-W. Qiu, A. Akbarzadeh, T. Han, and A. J. Danner, "Photorealistic rendering of a graded negative-index metamaterial magnifier," *New J. Phys.* **14**, 033024 (2012).
12. C. Y. Kim and R. Blake, "Psychophysical magic: rendering the visible 'invisible,'" *Trends Cogn. Sci.* **9**, 381–388 (2005).
13. J. C. Halimeh, R. Schmied, and M. Wegener, "Newtonian photorealistic ray tracing of grating cloaks and correlation-function-based cloaking-quality assessment," *Opt. Express* **19**, 6078–6092 (2011).
14. J. P. Lewis, "Fast normalized cross-correlation," *Vis. Interface* **10**, 120–123 (1995).
15. Z. Wang, A. C. Bovik, H. R. Sheikh, and E. P. Simoncelli, "Image quality assessment: from error visibility to structural similarity," *IEEE Trans. Image Process.* **13**, 1–14 (2004).
16. Equation (3) uses a L1 norm instead of a L2 norm because it showed better agreement with perceived invisibility in all our calculations. We attribute this behavior of L1 to a reduced spectrum smoothing, to robustness to data outliers, and to the analogy with "spot the differences" game.
17. A. B. Watson and A. J. Ahumada, Jr., "A standard model for foveal detection of spatial contrast," *J. Vis.* **5**(9):6, 717–740 (2005).
18. E. Peli, "Contrast sensitivity function and image discrimination," *J. Opt. Soc. Am. A* **18**, 283–293 (2001).
19. S. Daly, "The visible differences predictor: an algorithm for the assessment of image fidelity," in *Digital Image and Human Vision*, A. Watson, ed. (MIT, 1993), pp. 179–206.
20. ModelFest stimuli database, <http://vision.arc.n740asa.gov/modelfest/stimuli.html>.
21. Human face is the well known Lena image, which contains a rich mixture of detail, flat regions, shading, and texture for testing visual perception.